

DIEL AND SEASONAL PATTERNS OF TROPICAL FOREST CO₂ EXCHANGE

MICHAEL L. GOULDEN,^{1,3} SCOTT D. MILLER,¹ HUMBERTO R. DA ROCHA,² MARY C. MENTON,¹
HELBER C. DE FREITAS,² ADELAINE MICHELA E SILVA FIGUEIRA,² AND CLEILIM ALBERT DIAS DE SOUSA²

¹Department of Earth System Science, University of California, Irvine, California 92697-3100 USA

²Department of Atmospheric Sciences, University of São Paulo, São Paulo, Brazil

Abstract. We used eddy covariance to measure the net exchange of CO₂ between the atmosphere and an old-growth tropical forest in Pará, Brazil from 1 July 2000 to 1 July 2001. The mean air temperature and daily temperature range varied little year-round; the rainy season lasted from late December to around July. Daytime CO₂ uptake under high irradiance averaged 16–19 μmol·m⁻²·s⁻¹. Light was the main controller of CO₂ exchange, accounting for 48% of the half-hour-to-half-hour variance. The rate of canopy photosynthesis at a given irradiance was lower in the afternoon than the morning. This photosynthetic inhibition was probably caused by high evaporative demand, high temperature, an intrinsic circadian rhythm, or a combination of the three. Wood increment increased from January to May, suggesting greater rates of carbon sequestration during the wet season. However, the daily net CO₂ exchange measured by eddy covariance revealed the opposite trend, with greater carbon accumulation during the dry season. A reduction in respiration during the dry season was an important cause of this seasonal pattern. The surface litter was desiccated in the dry season, and the seasonal pattern of respiration appears to be a direct result of reduced forest floor decomposition during drought. In contrast, canopy photosynthesis was not directly reduced by the dry season, probably because deep rooting allows the forest to avoid drought stress

Key words: Amazonia; biosphere–atmosphere exchange; canopy photosynthesis; CO₂ exchange; eddy covariance; LBA; phenology; tropical forest.

INTRODUCTION

One of the goals of the Large-scale Biosphere–Atmosphere Experiment in Amazonia (LBA) is to understand how and why tropical forest CO₂ exchange varies diurnally and seasonally. Ecosystems take up CO₂ during photosynthesis and release it during autotrophic and heterotrophic respiration. The rates of ecosystem photosynthesis, respiration, and decomposition vary diurnally and seasonally in response to interactions between the physical environment (for example, irradiance and temperature) and the biota's physiology (for example, plant phenology and microbial basal metabolism). The challenge is to explain the diel and seasonal patterns of net CO₂ exchange by tropical forest based on the interactions between weather, photosynthesis, respiration, and decomposition.

Eddy covariance is a micrometeorological technique that provides half-hour observations of the net CO₂ exchange between a 10- to 1000-ha patch of land and the atmosphere (Baldocchi et al. 1988). Long-term eddy covariance data sets have been used to characterize the diel and seasonal patterns of CO₂ exchange by temperate deciduous forest (Wofsy et al. 1993, Greco and Baldocchi 1996, Goulden et al. 1996b), tem-

perate evergreen forest (Hollinger et al. 1994), and boreal forest (Fan et al. 1995, Black et al. 1996, Goulden et al. 1997, Jarvis et al. 1997). Analysis of eddy covariance observations provides useful information for identifying which physiological and physical processes play dominant roles in controlling CO₂ exchange. In turn, this information contributes to the development and improvement of models of ecosystem–atmosphere CO₂ exchange. While tropical forests are responsible for a quarter of global terrestrial GPP, published analyses of the patterns of tropical forest CO₂ exchange have been restricted to a couple of long-term (Malhi et al. 1998, Araújo et al. 2002) and short-term (Fan et al. 1990, Grace et al. 1996) data sets. There is a clear need for further data sets and analyses that describe and explain the temporal patterns of CO₂ exchange by tropical forest.

We used eddy covariance to measure the net exchange of CO₂ between the atmosphere and a primary tropical forest in Pará, Brazil from 1 July 2000 to 1 July 2001. In this paper, we analyze the responses of whole-forest photosynthesis and respiration to the physical environment from an ecophysiological perspective. We (1) introduce the site, experimental design, and data set; (2) describe the diel and seasonal patterns of weather and CO₂ exchange; (3) analyze the controls on the daily cycle of CO₂ exchange; (4) analyze the controls on the seasonal pattern of CO₂ exchange; and (5) summarize the importance of these

Manuscript received 25 November 2002; accepted 6 December 2002; final version received 30 January 2003. Corresponding Editor: D. S. Schimel. For reprints of this Special Issue, see footnote 1, p. S1.

³ E-mail: mgoulden@uci.edu

processes in controlling CO₂ exchange. A companion paper (Miller et al. 2004) discusses the site's annual carbon balance. A second companion paper (da Rocha et al. 2004) discusses the site's energy and water balances.

METHODS

Site

The measurements were made at the FLONA Tapajós km 83 Tower Site, ~70 km south of Santarem, Pará (3.01030° S, 54.58150° W). The site was in the Tapajós National Forest, with the nearest road 5 km east (the Santarem-Cuiba highway, BR-163). Access to the site was by a dirt road after turning off BR-163 near the km 83 post. The vegetation was closed tropical forest with canopy emergents on flat upland terrain (Hernandez Filho et al. 1993). The forest was semideciduous, with mostly evergreen and a few deciduous species. Forest extended 5 km to the east before reaching pasture on the far side of BR-163, 8 km to the south before reaching pasture, and 40 km to the north before reaching pasture. The site was on a flat plateau (the planalto) that extended many kilometers to the north, south, and east. The total relief within 1–2 km of the tower was ~10 m, with occasional 10–30 m deep stream gulleys farther from the tower. Forest continued 8 km west to the edge of the planalto before dropping to the Tapajós River, which was 14 km from the tower.

The site was selectively logged in September 2001 as part of a larger experiment. The emphasis in the current paper is on the CO₂ exchange by the old growth, undisturbed forest as measured before September 2001. All of the meteorological, tower flux, and litterfall observations reported here were made prior to logging. The logging removed only ~5% of the aboveground biomass, which created a patchwork of intact forest surrounding newly created gaps. The soil respiration measurements were made after the logging, in a large intact patch of forest that was ~50 m from the nearest gap. The wood increment measurements span the logging, which may confound their interpretation. However, the seasonal pattern of wood increment observed after the logging is similar to that observed before the logging, and also that observed in a nearby intact forest during the same period (Rice et al. 2004). Hence, we are confident that the limited use of data from after the cut does not compromise our conclusions.

Meteorological and tower flux

The flux measurements were made from a 67 m tall, 46 cm diameter tower (model 55G; Rohn, Peoria, Illinois, USA). The equipment at the tower top (64 m) was mounted on a winch-driven elevator (model TS-2000; Tower Systems, Watertown, South Dakota, USA) that was used periodically to lower the instruments to the forest floor for service. Additional instruments were mounted directly on the tower or on one of two 2-m

tripods installed on the forest floor. The data-acquisition computer and closed-path gas analyzers were operated in a pair of racks located in an air-conditioned hut 8 m south of the tower base. Power was provided by one of two 20-kVA diesel generators located 800 m south of the tower. The site was visited every week by a local employee to download data and every 4–6 mo, or as needed, by University of California, Irvine (UCI) and University of São Paulo (USP) personnel for maintenance or repair.

The data acquisition and control systems were automated, allowing extended periods of unattended operation. The data acquisition system used five data loggers (model CR10x or CR23x; Campbell Scientific, Logan, Utah, USA) in the following locations: tower top, tower base, IRGA rack, computer rack, and forest floor. The data loggers were connected by a coaxial network (Campbell Scientific model MD9) to a personal computer (Dell Computer, Austin, Texas, USA) that archived the raw data. The data loggers each ran individualized programs that managed local control and data acquisition, and prepared two types of data files: slow files with 30-min statistics and fast files with raw 4- or 0.5-Hz observations. The personal computer collected both slow and fast data from all data loggers every 4 min (Campbell Scientific model PC208), appending the most recent observations to separate slow and fast files for each data logger. The slow files were used to rapidly diagnose the equipment's operation; the fast files were used to prepare the final data sets.

The overall system was controlled by a data logger located in the computer rack (The Boss). The Boss operated continuously and was responsible for monitoring the generator voltage and tower data acquisition equipment, including the amount of traffic on the network. The Boss switched off all equipment following power failure, sequentially restarted the system when power returned, cycled the power to any data logger that failed to respond to a request from the computer, and rebooted the computer if there was no activity on the network.

The turbulent fluxes of sensible heat, latent heat, CO₂, and momentum at 64 m were determined with the eddy covariance technique (Baldocchi et al. 1988, Wofsy et al. 1993). The signals directly required for flux calculation were digitized and stored at 4 Hz. Wind and temperature were measured with a three-axis sonic anemometer pointed due east (Campbell Scientific). Winds from the east predominate at 64 m (Miller et al. 2004).

The molar densities of CO₂ and H₂O at 64 m were measured with two independent infrared gas analyzers (IRGAs). The first measurement was made by drawing 20–24 standard L/min of air through a closed-path IRGA (model LI7000 or, before December 2000, model LI6262; Li-Cor, Lincoln, Nebraska, USA) in the instrument hut. Air was drawn through a coarse poly-

ethylene screen inlet 50 cm above the sonic anemometer, down a 9.5 mm inner diameter, 75 m long, Teflon, PFA tube, and through a 1 μm pore, 142 mm diameter, Teflon filter. The sample tube was encased in an insulated heating bundle (model 2256; Unitherm, Cape Coral, Florida, USA) that maintained its entire length at 65°C to prevent condensation and reduce water vapor exchange with the wall. The pressure in the IRGA cell was actively controlled at 85 kPa (MKS Instruments, Andover, Massachusetts, USA). The IRGA reference cell was flushed with 1 standard L/min of CO₂- and H₂O-free air from a purge air generator (model GEN PGW 28 LC; Matheson, Montgomeryville, Pennsylvania, USA). The IRGA was calibrated daily by sequentially sampling purge air, CO₂ standard in air ($\pm 1\%$; Scott Marin, Riverside, California, USA), CO₂-free air (Scott Marin), and room air drawn through a thermoelectrically cooled condensing column at 16°C (Li-Cor LI610). The LI7000 absorptances were recorded and the gains, zeros, instrument nonlinearity, temperature, pressure, and effects of water vapor accounted for in subsequent processing (Li-Cor 2000). The second measurement of CO₂ and H₂O at 64 m was made with an open path IRGA (Li-Cor LI7500) positioned 40 cm south of the sonic anemometer.

The CO₂ fluxes for both the open- and closed-path IRGAs were calculated as the 30-min covariance of the vertical wind velocity (w) and the CO₂ mixing ratio (c). The time lag for the closed-path IRGA (approximately 11 s) was determined by maximizing the correlation between the fluctuations in air temperature (T) and c' . The fluxes were rotated to the plane with no mean vertical wind (McMillen 1988). Miller et al. (2004) compare the results from the open- and closed-path systems, and discuss the sensitivity of calculated flux to averaging time, detrending, and method of open-path density correction. All of the fluxes reported in the current manuscript were calculated using the closed-path IRGA with the sample-by-sample density correction for humidity. Parallel analyses using the fluxes calculated with the open-path IRGA yielded similar conclusions. In particular, the closed- and open-path IRGAs both indicated similar seasonal patterns of flux, with no discontinuity following the change in closed-path IRGA model in December 2000.

A third IRGA (Li-Cor LI7000 or, before December 2000, LI800) sequentially measured the densities of CO₂ and H₂O at 12 heights (0.1, 0.35, 0.7, 1.4, 3, 6, 10.7, 20, 35, 40, 50, and 64 m above the ground) every 48 min. An aliquot of air (4 standard L/min) was drawn through a 2 μm filter at each height, down 5.5 mm inner diameter polyethylene lined tubing (Furon Dekabon 1300; Saint-Gobain Performance Plastics, Wayne, New Jersey, USA), through a solenoid manifold in an enclosure at the base of the tower (Parker General Valve, Fairfield, New Jersey, USA), into the equipment hut, and through the IRGA cell. The pres-

sure in the IRGA cell was actively controlled at 83 kPa (MKS Instruments, Andover, Massachusetts, USA). The IRGA was calibrated for CO₂ and water vapor daily by sequentially sampling purge air, CO₂ standard in air ($\pm 1\%$; Scott Marin), CO₂-free air (Scott Marin), and 16°C dew-point air (Li-Cor LI610). The half-hourly change in CO₂ beneath 64 m (storage, Wofsy et al. 1993) was calculated by vertical integration and temporal differentiation. The eddy flux and storage observations were added to calculate the half-hourly net ecosystem exchange (NEE, Wofsy et al. 1993).

Observations of the physical environment were archived at 0.5 Hz. Precipitation at 64 m was measured with a tipping-bucket gauge (TE525; Texas Electronics, Dallas Texas, USA). Atmospheric pressure at 64 m was measured by the LI7500. Incoming and reflected photosynthetically active photon flux density (PPFD) at 64 m was measured with silicon quantum sensors (Li-Cor LI190). Net radiation at 64 m was measured with a thermopile net radiometer (REBS Q*7.1; REBS, Seattle Washington, USA). Incoming solar radiation at 64 m was measured with a thermopile pyranometer (model CM6; Kipp and Zonen, Delft, The Netherlands). Air temperatures at 64, 40, 10, and 2 m height were measured with ventilated thermistors (model 076B, Met One, Grants Pass, Oregon, USA; and model 107, Campbell Scientific). Horizontal wind speeds at 64, 50, and 40 m height were measured with cup anemometers (model 014; Met One). Soil temperatures at 19 locations from 0.02 to 2.5 m beneath the soil surface were measured with copper constantan thermocouples (Omega Engineering, Stamford, Connecticut, USA). Soil heat flux at 2-cm depth was measured with five flux plates (REBS HFT3.1). Soil moisture at 20 locations from 0.1 to 2.5 m beneath the soil surface was measured with water content reflectometers (Campbell Scientific CS615). Soil moisture content was calculated using calibration curves measured for the site by da Rocha et al. (2004). Litter moisture was measured using six fuel moisture probes positioned immediately above the forest floor (Campbell Scientific CS505).

Soil respiration was measured beginning in August 2001 with 15 automated chambers similar in design to Goulden and Crill (1997). The chambers were positioned in intact forest ~ 50 m east of the tower and ~ 50 m from the nearest logging-created gap. The chambers were sequentially sampled at 12-min intervals, and the soil respiration was calculated from the rate of CO₂ rise in each chamber.

Litter fall and wood increment

Litterfall, biomass, and wood increment were measured in an 18-ha block that extended 500 m east, 100 m west, 150 m south, and 150 m north of the tower (Miller et al. 2004). Wind was generally from the east, so this area included the region of forest most heavily sampled by eddy covariance, at least during daytime.

The 18-ha block was permanently marked with stakes at 25-m intervals, and the location and diameter of all trees with diameter at breast height (dbh) >35 cm was recorded in March 2000. Aboveground biomass was calculated as the mean of four allometric relations (Keller et al. 2001). Stainless steel dendrometer bands (Liming 1957) were placed on a subsample of 150 trees in October 2000. The dendrometer sample included a representative sampling of species and an overrepresentation of large trees. The dendrometers were measured at 6-wk intervals using digital calipers, and the biomass calculated as the mean of four allometric relations (Keller et al. 2001). The woody increment was then scaled to ground area by multiplying the dendrometer subsample's fractional biomass gain by the 18-ha block's aboveground biomass density. This scaling should provide a good measure of the seasonal pattern of wood increment regardless of whether the proportional woody increment of the dendrometer subsample matches the overall increment in the block.

Litter was collected biweekly from 30 1-m² traps, which were arrayed at 25-m intervals along two east-west transects in the 18-ha block. The litter was returned to the lab where it was sorted, air dried, and weighed. A subsample was dried in an oven, and the air-dried weights were corrected to oven-dried weight. Prior to oven drying, the subsample's leaf area was determined using a computer scanner and image processing software. The area of leaf litter collected during each sampling was calculated using the relationship between weight and area measured for the subsample.

Uncertainty and sign convention

A companion paper (Miller et al. 2004) discusses the accuracy of the half-hour and annually integrated CO₂ exchange for this data set. Eddy covariance is considered most reliable when used for analyses that require temporal precision rather than absolute accuracy, and also when used for analyses based on individual half-hour fluxes rather than daily or annually integrated flux (Goulden et al. 1996b). The additional uncertainty at longer time step is caused by day to night biases in atmospheric transport. Daily and annual sums represent the difference between day uptake and night efflux. Relatively small biases from day to night, such as a systematic underestimation of flux at night relative to day, can create large uncertainty in the absolute accuracy of daily or annual sums. Miller et al. (2004) found that the annual integrated flux was extremely sensitive to the treatment of day-to-night bias, increasing by ~4 Mg·ha⁻¹·yr⁻¹ when a u^* filter was applied (u^* refers to the friction velocity, see Miller et al. 2004 and Goulden et al. 1996b for details).

Uncertainties associated with the treatment of calm nights are considered less important when analyzing temporal trends, since the effect of day to night bias is thought to be constant from one day to the next.

Miller et al. (2004) found that the seasonal pattern of daily carbon balance was comparatively insensitive to whether or not a u^* filter was applied. The u^* filter increased the daily net CO₂ exchange by ~15 kg C·ha⁻¹·d⁻¹ throughout the year, resulting in a large increase in the annual integral, but no major change in the seasonal pattern of daily CO₂ exchange (compare the derivatives of curve 1 and curve 5 in Fig. 4 of Miller et al. 2004). Because the analysis presented here focuses on the relative changes in CO₂ exchange with time (diel and seasonal patterns), we did not attempt to correct the data for uncertainties associated with day to night measurement bias. As a result, the absolute rates of apparent daily carbon accumulation reported here likely overestimate the true rates of daily carbon accumulation by ~15 kg C·ha⁻¹·d⁻¹. Likewise, the rates of respiration reported here, which include observations of NEE during calm nights, likely underestimate the true rates of respiration by ~3 μmol·m⁻²·s⁻¹. Our analysis is intended to provide an accurate determination of the diel and seasonal patterns of CO₂ exchange, rather than the absolute rates of respiration and daily carbon balance.

Eddy covariance observations are usually presented using the atmospheric scientist's sign convention, with a negative flux indicating net downward transport of CO₂. Photosynthesis is therefore defined as a negative flux, which is opposite the sign convention used by ecologists. The result can be confusing, especially when relative changes in CO₂ exchange are discussed. In this paper we use the atmospheric scientist's sign convention in all CO₂ flux figures, but discuss temporal changes using positive sign conventions for respiration, photosynthesis and net CO₂ uptake. Consequently, we describe an increase in photosynthesis and CO₂ uptake with increasing irradiance, even though the associated figures shows that the net CO₂ exchange becomes more negative with increasing irradiance. Inconsistency of this type is difficult to avoid, since either uptake or efflux must be defined as a negative flux in figures, whereas both respiration and photosynthesis are normally discussed as processes with positive sign.

RESULTS AND DISCUSSION

We installed the equipment and began measurements in late June 2000. Valid measurements of meteorology were made during 16 400 half-hours from 1 July 2000 to 1 July 2001, or 93% of the time (Fig. 1). Valid measurements of NEE were made during 12 700 half-hours from 1 July 2000 to 1 July 2001, or 72% of the time (Fig. 2). Extended gaps occurred in October 2000 and April 2001 when the tower-top data logger malfunctioned, January 2001 when the power failed during a severe storm, and April 2001 when the sonic anemometer malfunctioned. Shorter gaps in NEE occurred during calibrations and when the sonic anemometer measurement was compromised by rain.

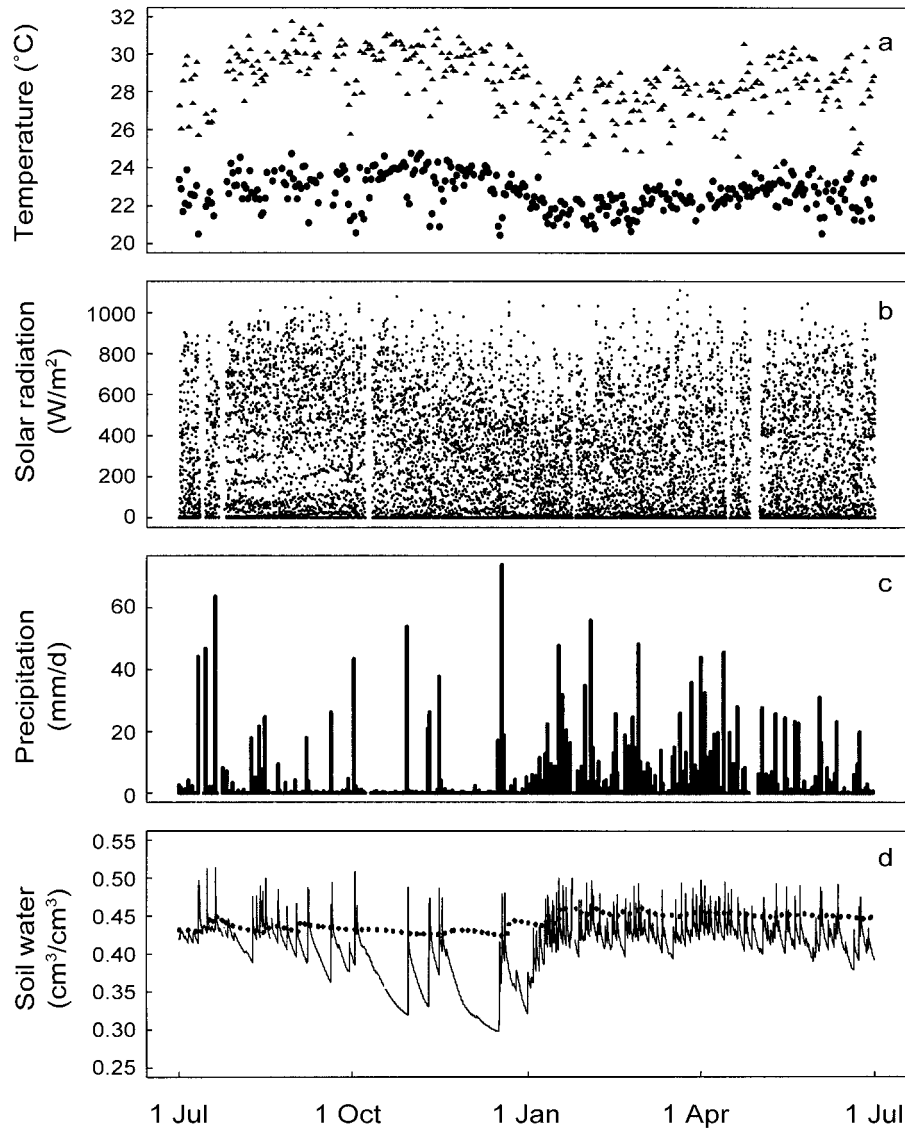


FIG. 1. (a) Maximum (triangles) and minimum (circles) daily air temperature ($^{\circ}\text{C}$) at 64 m height above the FLONA Tapajós km 83 Tower Site from 1 July 2000 to 1 July 2001. (b) Thirty-minute mean solar radiation at 64 m height (W/m^2). (c) Daily rainfall at 64 m height (mm/d). (d) Soil water content at 10 cm (solid line) and 225 cm (heavy dashed line) depth (cm^3/cm^3).

Seasonal patterns of meteorology

The mean air temperature and daily temperature range at 64 m varied little year-round (Fig. 1a). The absolute maximum 30-min temperature was 31.7°C and the absolute minimum 30-min temperature was 20.4°C . Comparatively cool air temperatures in December and January coincided with a cloudy period (Fig. 1b) at the beginning of the rainy season (Fig. 1c). Aside from this cloudy period, peak incoming solar radiation was generally consistent year-round, with modest increases around the equinoxes and decreases around the solstices (Fig. 1b, see also da Rocha et al. 2004).

The rainy season lasted from late December to around July (Fig. 1c). The total rainfall was over 200 cm. Almost all of the rain occurred during brief, 5–15 min long storms that dropped <10 mm of rain. The short duration of rainfall indicates these storms were small and localized. The surface soil was above field capacity throughout much of the rainy season, when one or more storms a day saturated the shallow layers (Fig. 1d). The dry season was interrupted by several storms, with extended dry periods in October and November through December (Fig. 1c). The soil throughout the profile remained surprisingly moist year-round, with a volumetric content above $0.3 \text{ cm}^3/\text{cm}^3$ (Fig. 1d).

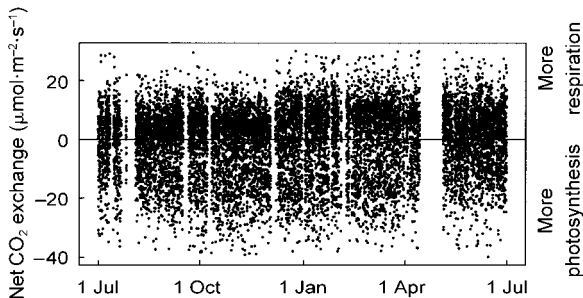


FIG. 2. Net ecosystem exchange of CO₂ (NEE; $\mu\text{mol}\cdot\text{m}^{-2}\cdot\text{s}^{-1}$) during 12 700 half-hours from 1 July 2000 to 1 July 2001. NEE was calculated by adding the turbulent flux at 64 m measured by eddy covariance and the change in storage beneath 64 m. Positive exchange indicates a net input of CO₂ to the atmosphere.

The soil water content at 2.25 m was relatively constant year-round, with modest declines during long dry periods and increases a few days after heavy storms.

Diel patterns of meteorology and CO₂ exchange

The sun rose at 0600 hours local time and set at 1800 hours local time (Fig. 3a). The peak PPFD was $\sim 2000 \mu\text{mol}\cdot\text{m}^{-2}\cdot\text{s}^{-1}$, though average PPFD was only $\sim 60\%$ of peak due to frequent cloud cover. The afternoons were slightly cloudier than the mornings. Air temper-

ature at 64 m began to increase shortly after sunrise and reached a peak shortly after noon (Fig. 3b). Vertical mixing at 64 m, as indicated by friction velocity (u^*), was low at night before increasing rapidly with the sun in the morning and peaking before noon (Fig. 3d). Vertical mixing declined gradually in the afternoon until 1500 hours local time and then rapidly from 1500 to 1800 hours local time with sunset.

The net ecosystem exchange (NEE) was calculated as the sum of turbulent CO₂ exchange at 64 m determined by eddy covariance (eddy flux), and the change in CO₂ beneath the tower top determined by measuring the CO₂ profile (storage). Both the eddy flux and storage made large contributions to NEE (Fig. 3c), and both must be measured for analyses of short-term patterns of CO₂ exchange.

The CO₂ uptake by the ecosystem, as indicated by a less positive or more negative NEE, increased rapidly after sunrise, with photosynthesis compensating ecosystem respiration on average at 0700 hours local time and a mean irradiance of $300 \mu\text{mol}\cdot\text{m}^{-2}\cdot\text{s}^{-1}$. CO₂ uptake continued to increase with sunlight, before peaking at an average of $19 \mu\text{mol}\cdot\text{m}^{-2}\cdot\text{s}^{-1}$ at 1000 hours local time, ~ 2 h before maximum sunlight (Fig. 3a, c). CO₂ uptake then declined steadily through the afternoon, passing the compensation point at 1630 hours local time when the mean irradiance was $300 \mu\text{mol}\cdot\text{m}^{-2}\cdot\text{s}^{-1}$. These rates

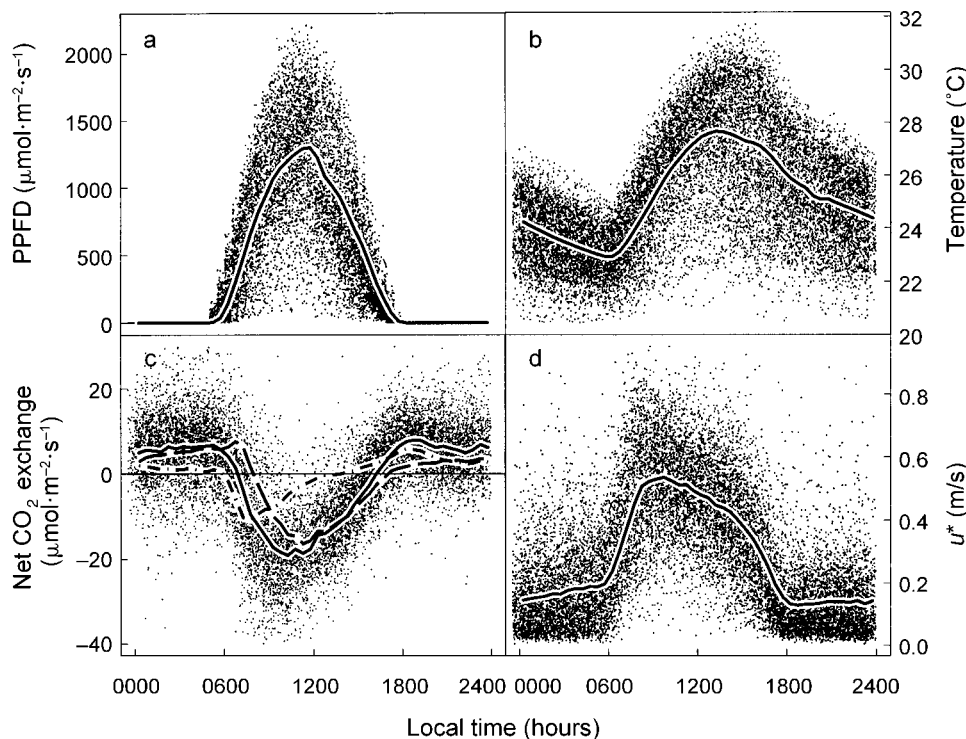


FIG. 3. (a) Daily changes in incident PPFD ($\mu\text{mol}\cdot\text{m}^{-2}\cdot\text{s}^{-1}$), (b) air temperature at 64 m ($^{\circ}\text{C}$), (c) net CO₂ exchange (NEE; $\mu\text{mol}\cdot\text{m}^{-2}\cdot\text{s}^{-1}$), and (d) friction velocity at 64 m (u^* ; m/s). Individual points are half-hourly observations. The time of each observation was randomly changed by as much as 15 min to separate the points. Lines are means for each half hour. The solid line in (c) is NEE, the coarse dashed line is the eddy flux, and the fine dashed line is the storage.

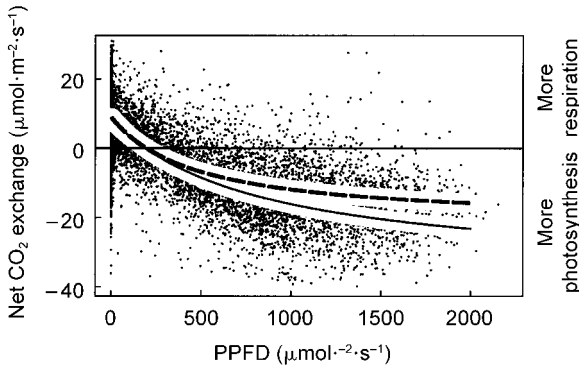


FIG. 4. Net CO_2 exchange ($\mu\text{mol}\cdot\text{m}^{-2}\cdot\text{s}^{-1}$) as a function of incident photosynthetically active photon flux density (PPFD; $\mu\text{mol}\cdot\text{PAR}\cdot\text{m}^{-2}\cdot\text{s}^{-1}$). The best fit for morning periods (before 1115 hours local time with $\text{PPFD} > 10 \mu\text{mol}\cdot\text{m}^{-2}\cdot\text{s}^{-1}$; solid line) was net CO_2 exchange = $8.4 + (-44.7\text{PPFD}) / (816 + \text{PPFD})$, $n = 3060$. The best fit for afternoon periods (after 1115 hours local time with $\text{PPFD} > 10 \mu\text{mol}\cdot\text{m}^{-2}\cdot\text{s}^{-1}$; dashed line) was net CO_2 exchange = $9.1 + (-30.7\text{PPFD}) / (469 + \text{PPFD})$, $n = 2970$.

of uptake are similar to those reported for other tropical forest (Grace et al. 1996, Malhi et al. 1998). For comparison, this uptake is similar to that reported for temperate deciduous forest (Goulden et al. 1996b), and about 50% higher than that reported for evergreen boreal forest (Goulden et al. 1997). Nocturnal respiration averaged $6\text{--}7 \mu\text{mol}\cdot\text{m}^{-2}\cdot\text{s}^{-1}$ throughout the night, following a possible modest peak shortly after dusk (Fig. 3c). Nocturnal respiration was similar to that reported for other tropical forest (Grace et al. 1996, Malhi et al. 1998). Respiration was about twice that reported for both temperate deciduous forest (Goulden et al. 1996b) and evergreen boreal forest (Goulden et al. 1997) (see *Methods: Uncertainty and sign convention* and Miller et al. [2004] for a discussion of bias in the absolute accuracy of the nocturnal respiration measurements).

Controls on diel pattern of CO_2 exchange

Irradiance was the main controller of net CO_2 exchange, with an r^2 of 0.48 (Fig. 4). CO_2 uptake increased in the morning with an initial slope of $0.055 \mu\text{mol}\cdot\text{CO}_2/\mu\text{mol}\cdot\text{PAR}$ before beginning to saturate at $500\text{--}1000 \mu\text{mol}\cdot\text{PAR}\cdot\text{m}^{-2}\cdot\text{s}^{-1}$. The shape of the light curve was similar to that reported for other tropical forest (Malhi et al. 1998, Fan et al. 1990). The shape of the light curve was also similar to that reported for temperate deciduous forest, which began to saturate at $500\text{--}1000 \mu\text{mol}\cdot\text{PAR}\cdot\text{m}^{-2}\cdot\text{s}^{-1}$ after an initial slope of $0.055 \mu\text{mol}\cdot\text{CO}_2/\mu\text{mol}\cdot\text{PAR}$ (Goulden et al. 1996b), and also evergreen boreal forest which saturated at $500\text{--}600 \mu\text{mol}\cdot\text{PAR}\cdot\text{m}^{-2}\cdot\text{s}^{-1}$ after an initial slope of $0.040 \mu\text{mol}\cdot\text{CO}_2/\mu\text{mol}\cdot\text{PAR}$ (Goulden et al. 1997). Likewise, the dominance of irradiance in controlling net CO_2 uptake is similar to reports for a range of forest types (Jarvis and Leverenz 1983, Hollinger et al. 1994,

Ruimy et al. 1995, Goulden et al. 1997), including tropical forest (Malhi et al. 1998).

CO_2 uptake at a given irradiance was lower in the afternoon than in the morning (Figs. 3a, c, 4). The residual CO_2 exchange under high irradiance, which was calculated by subtracting the NEE expected based on a curve fit using morning observations from observed NEE, remained near zero in the morning, before increasing to $5\text{--}8 \mu\text{mol}\cdot\text{m}^{-2}\cdot\text{s}^{-1}$ in the afternoon (Fig. 5). A more positive residual NEE indicates the observed CO_2 uptake was less than would be expected based on irradiance, which, in turn, indicates a reduction in photosynthesis or an increase in respiration.

Afternoon declines in leaf-level gas exchange have been reported for many ecosystems (Larcher 1995), including tropical forest (Koch et al. 1994, Malhi et al. 1998, Zotz and Winter 1996). Investigators have attributed afternoon depression to many causes including stomatal response to VPD or low leaf-water potential, photosynthetic effects of elevated temperature, starch and metabolite accumulation, intrinsic circadian rhythm, and increases in leaf, plant, or soil respiration due to elevated temperature (Jones 1992, Larcher 1995). As a practical matter, these factors covary over the day and are difficult to separate in observational data. Nonetheless, the extent of our data set allowed us to isolate and separately consider some of these factors.

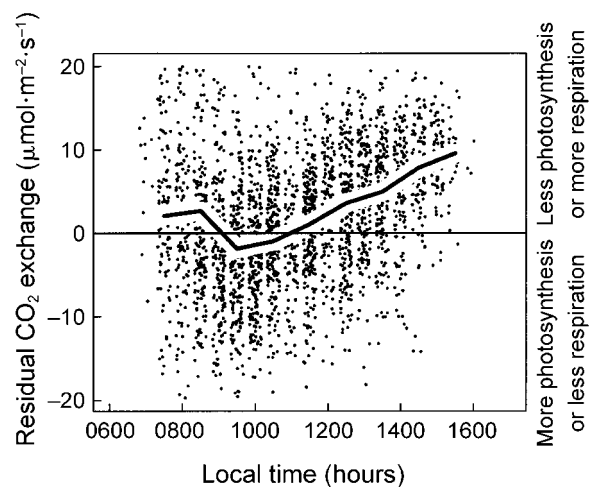


FIG. 5. Residual NEE (net ecosystem exchange; $\mu\text{mol}\cdot\text{m}^{-2}\cdot\text{s}^{-1}$) as a function of local time during bright periods ($\text{PPFD} > 800 \mu\text{mol}\cdot\text{m}^{-2}\cdot\text{s}^{-1}$). Residual NEE was calculated by subtracting the NEE expected based on a curve fit using morning observations (before 1100 hours local time; $6.7 + [-33.1(\text{PPFD})] / [593 + \text{PPFD}]$) from the observed NEE. A more positive residual NEE indicates the observed CO_2 uptake (photosynthesis) was less than would be expected based on irradiance. The time of each individual observation was randomly changed by as much as 15 min to separate the points. The thick line shows the mean residual NEE for each hour.

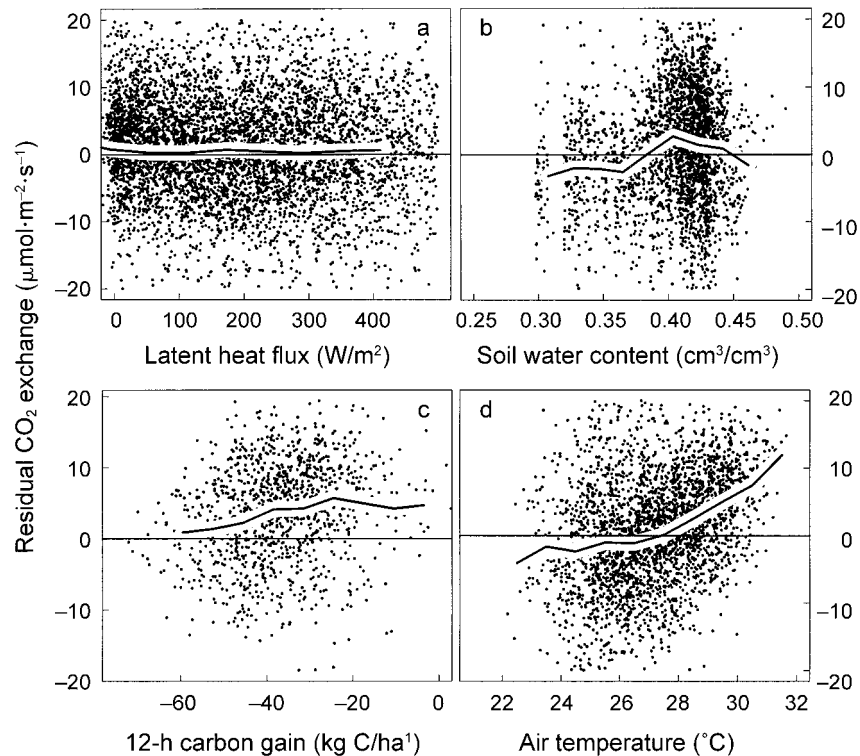


FIG. 6. Residual NEE (net ecosystem exchange; $\mu\text{mol}\cdot\text{m}^{-2}\cdot\text{s}^{-1}$) as a function of (a) evaporation (latent heat flux in W/m^2), (b) surface soil water content (cm^3/cm^3), (c) carbon accumulated in most recent 12 h ($\text{kg C}/\text{ha}$), and (d) air temperature at 64 m ($^{\circ}\text{C}$). Residual NEE was calculated as in Fig. 5. Panel (a) includes all periods with $\text{PPFD} > 100 \mu\text{mol}\cdot\text{m}^{-2}\cdot\text{s}^{-1}$; panels (b), (c), and (d) include only observations during bright periods ($\text{PPFD} > 800 \mu\text{mol}\cdot\text{m}^{-2}\cdot\text{s}^{-1}$). A more positive residual NEE indicates that observed photosynthesis was less than would be expected based on irradiance. Points above the horizontal lines indicate less photosynthesis or more respiration; conversely, points below the horizontal lines indicate more photosynthesis or less respiration. Carbon accumulated in most recent 12 h was calculated by summing the NEE during the most recent 12 h after setting nocturnal CO_2 exchange to zero.

A comparison of morning and afternoon light curves (Fig. 4) indicated that the afternoon decline in CO_2 uptake resulted from a change in photosynthesis (mean CO_2 uptake for $\text{PPFD} > 1000 \mu\text{mol PAR}\cdot\text{m}^{-2}\cdot\text{s}^{-1}$ was $17.9 \mu\text{mol}\cdot\text{m}^{-2}\cdot\text{s}^{-1}$ in the morning and $12.1 \mu\text{mol}\cdot\text{m}^{-2}\cdot\text{s}^{-1}$ in the afternoon) rather than a change in respiration (respiration determined by extrapolating the light curves was $8.4 \mu\text{mol}\cdot\text{m}^{-2}\cdot\text{s}^{-1}$ in the morning and $9.1 \mu\text{mol}\cdot\text{m}^{-2}\cdot\text{s}^{-1}$ in the afternoon).

The significance of low afternoon leaf water potentials (Williams et al. 1998) was discounted because of the poor relationship between residual NEE and both evapotranspiration (latent heat flux; Fig. 6a) and soil water content (Fig. 6b). Assuming steady state water flow and constant plant and soil hydraulic resistance, leaf water potential is proportional to transpiration and soil water potential (Jones 1992). Residual NEE indicated that canopy photosynthesis was constant with both increasing evapotranspiration (Fig. 6a) and decreasing soil water (Fig. 6b), implying that afternoon leaf desiccation was not responsible for the afternoon decline in photosynthesis. The degree of afternoon canopy photosynthetic decline did not increase in the dry

season, and there was no evidence of increased midday photosynthetic depression with drought. Likewise, residual NEE was not related to the recent accumulation of carbon (Fig. 6c), and, if anything, photosynthesis was greater than expected on afternoons with a particularly favorable carbohydrate status.

Residual NEE was comparatively well correlated with air temperature (Fig. 6d), though the relationship accounted for only a few percent of the remaining variance. Residual NEE increased to $8\text{--}12 \mu\text{mol}\cdot\text{m}^{-2}\cdot\text{s}^{-1}$ at air temperatures above 30°C , indicating a large decline in photosynthesis. Air temperature, leaf temperature, vapor pressure deficit, and time of day were tightly correlated with each other. We conclude that the afternoon decline in CO_2 uptake resulted from either stomatal closure in response to evaporative demand, or a change in photosynthetic biochemistry with elevated temperature, or a circadian rhythm, or a combination of mechanisms. However, we are unable to determine the relative importance of these mechanisms.

The effect of the physical environment, especially light, on forest physiology accounted for about half of the half-hour to half-hour variation in the diel pattern

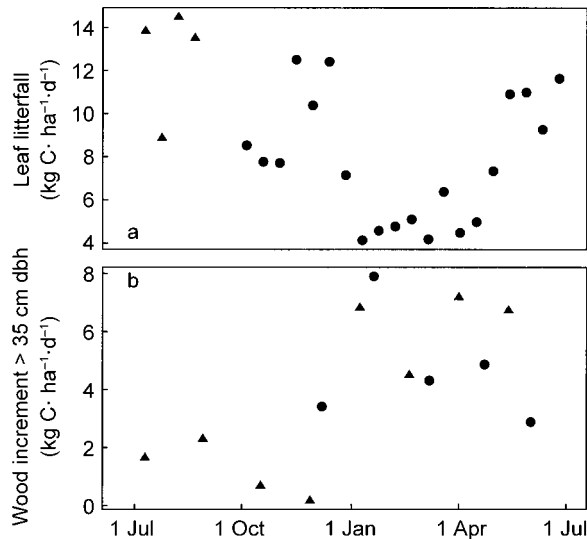


FIG. 7. Seasonal changes in (a) leaf litterfall ($\text{kg C} \cdot \text{ha}^{-1} \cdot \text{d}^{-1}$) and (b) gross wood increment by trees with a diameter at breast height (dbh) > 35 cm. Points in (a) are means for 30 1-m^2 traps located upwind of the eddy covariance tower collected biweekly plotted against the middle date between samplings. Points in (b) are means calculated using four allometric equations for 150 trees equipped with dendrometer bands measured at 6-wk intervals and plotted against the middle date between observations. Filled circles were observed before 1 July 2001. Filled triangles were observed after 1 July 2001.

of CO_2 flux. The remaining variance in CO_2 flux was likely a result of measurement uncertainty, including variability caused by the sampling of turbulence for the covariance calculation, variability caused by the sampling of profile CO_2 for the storage calculation, and spatial heterogeneity.

Seasonal patterns of litterfall and wood increment

Litterfall increased and wood increment decreased from May to December, a period that roughly coincided with the dry season (Figs. 1c, d, 7). The seasonal patterns of litterfall and wood increment, and the absolute rates of litterfall, were similar to those reported for nearby undisturbed forest during the same period (Rice et al. 2004). Likewise, the absolute rates of gross wood increment were similar to those reported by Rice et al. (2004), after accounting for wood production by trees with $\text{dbh} < 35$ cm.

We initially attributed the seasonal patterns of litterfall and wood increment to a direct effect of soil drought on leaf area index (LAI), canopy photosynthesis, and wood growth, as has been reported for other Amazonian forest (Malhi et al. 1998, Williams et al. 1998). However, a closer look indicated that the decrease in wood growth and increase in leaf senescence preceded the onset of the dry season (Figs. 1c, d, 7), implying that these were genetically programmed adaptations, as opposed to direct responses to drought

stress. The increase in leaf fall began in May and the decrease in wood increment began in June, whereas frequent rainfall continued until July, and soil water content remained high until August.

In fact, the forest appeared to avoid severe drought stress in the 2000 dry season despite continued high evapotranspiration and long periods without rainfall (Figs. 1c, 2, 6b; da Rocha et al. 2004). The rate of soil water withdrawal at the end of long drying cycles was approximately equal at both the soil surface and 2.25 m depth, with marked diel patterns at all depths (Fig. 1d), indicating that deep rooting allowed the trees to withdraw water evenly from a large volume of soil (Nepstad et al. 1994, da Rocha et al. 2004). Moreover, da Rocha et al. (2004) present evidence of hydraulic lift, which helped keep the upper soil moist despite the lack of rain (above $0.3 \text{ cm}^3/\text{cm}^3$; Fig. 1d) and may have increased the efficiency with which the trees exploited the soil water reserves. The seasonal pattern of leaf senescence appears to be an evolved response that anticipates the annual dry season, and is probably triggered by a cue other than soil water status. This phenomenon is consistent with that reported by Wright and Cornejo (1990), who observed that irrigation did not reduce the rate of dry-season litterfall in a Panamanian rainforest.

Seasonal pattern of canopy photosynthesis

Residual NEE decreased from October to April and increased from May to September, indicating that canopy photosynthesis under high irradiance was $5\text{--}10 \mu\text{mol} \cdot \text{m}^{-2} \cdot \text{s}^{-1}$ greater from October to April than from May to September (Fig. 8a). The May decline in photosynthesis at a given light level did not result directly from stomatal closure due to soil drought, since it preceded the beginning of the dry season (Figs. 1c, d, 8a). Likewise, the October increase in photosynthesis did not result from the relief of drought stress, since it preceded the resumption of frequent rain. Rather, the seasonal pattern of residual NEE appears related to the seasonal changes in leaf litterfall (Fig. 8b), and a probable change in leaf area index (LAI).

Direct observations of the seasonal pattern of LAI are unavailable, but anecdotal observations, combined with Fig. 8, provide a consistent picture. Canopy photosynthesis began to decrease in April (Fig. 8a), about one month before the increase in litterfall (Fig. 8b) and three months before the onset of the dry season (Fig. 1c, d). We believe the April decrease in photosynthesis was a result of the onset of leaf senescence, which resulted in increased litterfall that began soon after. Photosynthesis was reduced but constant and litterfall was high during the early dry season. We believe this period was marked by leaf turnover, and a relatively low canopy LAI caused by continual leaf growth and senescence. Photosynthesis increased from October to December, and leaf drop declined in December. We

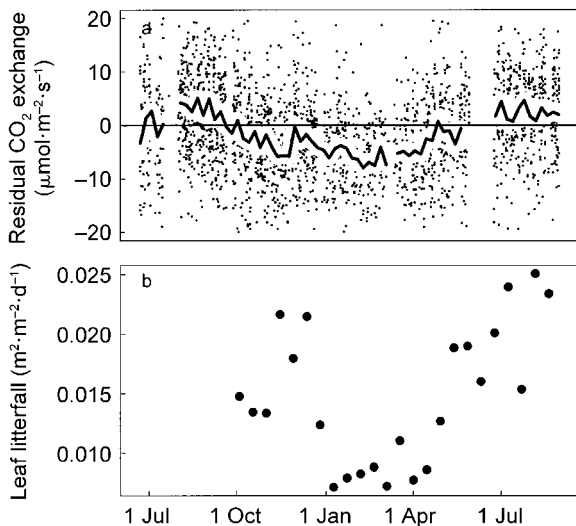


FIG. 8. (a) Residual NEE (net ecosystem exchange; μmol·m⁻²·s⁻¹) during bright periods from 1 July 2000 to 1 July 2001, and (b) leaf litterfall (m²·m⁻²·d⁻¹). Residual NEE was calculated as in Fig. 5. A more positive residual NEE indicates that observed CO₂ uptake (photosynthesis) was less than would be expected based on irradiance. Points above the horizontal line in (a) indicate less photosynthesis or more respiration; conversely, points below the line indicate more photosynthesis or less respiration. The individual points in (a) are half-hourly residual NEEs when the PPFD was >800 μmol·m⁻²·s⁻¹. The plotted curve in (a) shows the residual NEE during 5-d intervals. Points in (b) are means for 30 1-m² traps located upwind of the eddy covariance tower collected biweekly plotted against the middle date between samplings.

believe this period was marked by an increase in LAI caused by continual leaf growth and a decline in leaf senescence. These patterns are consistent with anecdotal observations of leaf growth and senescence at the site during 2000 and 2001.

Seasonal pattern of respiration

Average nocturnal CO₂ efflux, a measure of ecosystem respiration, was 2 μmol·m⁻²·s⁻¹ lower in the dry season than the wet season (Fig. 9). The measurements of nocturnal CO₂ efflux were noisy, as is typical above

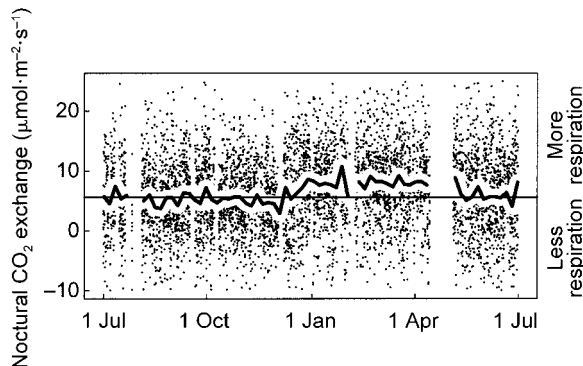
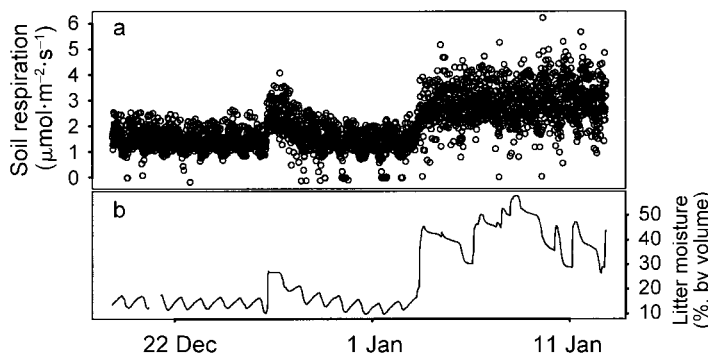


FIG. 9. Nocturnal CO₂ efflux (μmol·m⁻²·s⁻¹) from 1 July 2000 to 1 July 2001. The individual points are half-hourly NEEs when the PPFD was <10 μmol·m⁻²·s⁻¹. The line shows the mean nocturnal CO₂ efflux during 5-d intervals.

tall forest. The occurrence of individual nocturnal measurements with apparent CO₂ uptake is a result of this variability, rather than CO₂ fixation.

The surface litter became quite dry in the dry season, and the seasonal pattern of respiration appears to be a direct result of reduced forest floor decomposition during drought (Goulden et al. 1996a, Savage and Davidson 2001). This explanation is consistent with the rapid increase in respiration with rain observed by eddy covariance in December 2000 (Figs. 1c, d, 9), and also with the rapid increase in soil respiration immediately following litter rehydration observed by the automated chambers in December 2001 (Fig. 10). Soil respiration was relatively low late in the 2001 dry season, and increased by ~2 μmol·m⁻²·s⁻¹, or ~20 kg C·ha⁻¹·d⁻¹, with rainfall at the start of the wet season. Prior to the start of the wet season, soil respiration increased immediately after a 0.23-cm rain on 26 December moistened the litter layer (Fig. 10a). Respiration subsequently declined back to the original rate, following a pattern that paralleled the hydration of wooden dowels placed immediately above the litter layer (Fig. 10b). Respiration increased markedly and remained high with the start of the rainy season on 3 January. We attribute the rapid increase in soil respiration following rainfall to

FIG. 10. (a) Soil respiration (μmol·m⁻²·s⁻¹) and litter moisture (percentage moisture content by volume) at the transition from dry to wet season in December 2001 and January 2002. Points are individual rates of soil CO₂ efflux measured with one of 15 automated chambers. Litter moisture is the mean for six fuel moisture probes located immediately above the forest floor. The wet season began on 3 January 2002.



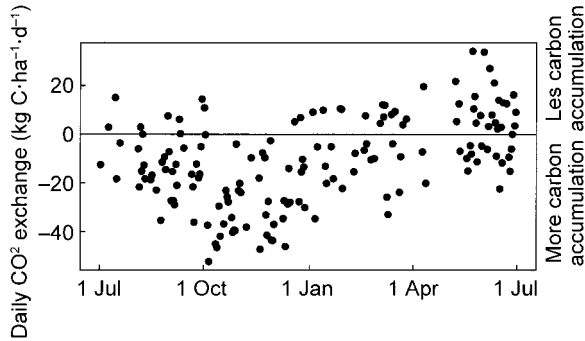


FIG. 11. Daily net CO_2 exchange ($\text{kg C}\cdot\text{ha}^{-1}\cdot\text{d}^{-1}$) at the FLONA Tapajós Logged Forest Tower Site from 1 July 2000 to 1 July 2001. Daily sums were calculated without correcting for calm periods (see *Methods*).

the relief of microbial water stress within the litter layer.

Seasonal pattern of net CO_2 exchange

Daily carbon balance (kg C/ha gained or lost per day) is the relatively small difference between CO_2 uptake during daytime and CO_2 efflux at night. Modest shifts in daytime uptake or nighttime efflux that are too small to notice when individual half-hour NEE observations are plotted (Fig. 2) may nonetheless cause large seasonal shifts in daily carbon accumulation. The site's daily carbon balance changed seasonally, with a modest average apparent carbon accumulation of $20 \text{ kg C}\cdot\text{ha}^{-1}\cdot\text{d}^{-1}$ at the beginning of the dry season (July through September), a large apparent carbon accumulation of $40 \text{ kg C}\cdot\text{ha}^{-1}\cdot\text{d}^{-1}$ later in the dry season (October through December), and little or no apparent carbon accumulation in the wet season (Fig. 11, see *Methods: Uncertainty and sign convention* and Miller et al. (2004) for a discussion of bias in the absolute accuracy of the calculated daily carbon balances). Most of the day-to-day scatter in daily carbon balance within a season was related to variation in sunlight, with greater uptake on sunnier days.

The seasonal pattern in daily carbon balance (Fig. 11) was opposite what we expected based on the observations of wood increment (Fig. 7). The wood increment suggested that carbon accumulation would decline in the dry season, reaching a minimum from June through December. However, carbon accumulation increased during the dry season, reaching a maximum in November and December (Fig. 11). Hence, daily carbon balance is not controlled by the accumulation of carbon in the relatively slow-turnover pool of woody biomass. Rather, daily carbon balance appears more closely related to changes in the amounts of carbon in relatively fast turnover pools, such as live and dead leaves.

Daily carbon balance (Fig. 11) is a function of the trends in residual canopy photosynthesis (Fig. 8) and

respiration (Figs. 9, 10). The residual daytime CO_2 exchange was $5\text{--}10 \mu\text{mol}\cdot\text{m}^{-2}\cdot\text{s}^{-1}$ greater from October to April than from May to September, which equals $\sim 20\text{--}40 \text{ kg C}\cdot\text{ha}^{-1}\cdot\text{d}^{-1}$ if summed 12 h/d (Fig. 8). Average nocturnal CO_2 efflux was $2 \mu\text{mol}\cdot\text{m}^{-2}\cdot\text{s}^{-1}$ lower in the dry season than the wet season, which equals $\sim 20 \text{ kg C}\cdot\text{ha}^{-1}\cdot\text{d}^{-1}$ if summed over 24 h/d (Fig. 9). Hence, the forest accumulated carbon at the greatest rate from October to December ($\sim 40 \text{ kg C}\cdot\text{ha}^{-1}\cdot\text{d}^{-1}$; Fig. 11), a period when respiration was low (reduced by $\sim 20 \text{ kg C}\cdot\text{ha}^{-1}\cdot\text{d}^{-1}$; Fig. 9) and residual canopy photosynthesis was high (increased by $\sim 20\text{--}40 \text{ kg C}\cdot\text{ha}^{-1}\cdot\text{d}^{-1}$; Fig. 8). This change in carbon balance probably reflects a change in the amount of carbon in the combined pool of live and dead leaves. This pool apparently gains carbon in the dry season, when decomposition declines and leaf growth accelerates, and loses carbon in the wet season, when decomposition accelerates and leaf growth declines.

We attribute the seasonal changes in respiration (Fig. 9) to the onset and relief of microbial water stress within the litter layer (Fig. 10). Hence, the dry season apparently has a greater effect on microbial decomposition than on tree photosynthesis. The trees at the site were sufficiently deeply rooted to escape drought stress, whereas litter decomposition was curtailed by desiccation. The seasonal pattern of net CO_2 exchange (Fig. 11) therefore results from a fundamental difference in the ways higher plants and microbes cope with the dry season. Trees are complex organisms that have evolved morphological (deep rooting), physiological (stomatal control), and phenological (leaf growth and senescence) strategies to avoid drought stress. In contrast, microbes are simple organisms with large surface area to volume ratios, which has limited the evolution of strategies for avoiding drought stress. Instead, the litter-layer microbes at the site apparently cope with the dry season by rapidly increasing or decreasing metabolism in response to hydration. Photosynthesis and plant phenology are relatively unaffected, and decomposition is strongly affected, by the dry season. These trends cause seasonal changes in the daily net CO_2 exchange and the amount of carbon in live and dead leaves.

Overview of diel and seasonal patterns of CO_2 exchange

Five aspects of forest physiology are important for understanding the forest's diel and seasonal patterns of CO_2 exchange: (1) the response of canopy photosynthesis to light, (2) the afternoon reduction in canopy photosynthesis at a given irradiance, (3) the seasonal patterns of LAI and canopy photosynthesis at a given irradiance, (4) the vegetation's ability to avoid drought stress, and (5) the effect of the dry season on decomposition.

Light was the main controller of half-hour CO₂ exchange, accounting for 48% of the half-hour-to-half-hour variance (Figs. 3a, c, 4). An accurate representation of the response of canopy photosynthesis to light is needed to accurately predict the diel pattern of CO₂ exchange. This response is a function of leaf gas exchange and the pattern of light interception by the canopy (Jarvis and Leverenz 1983, Ruimy et al. 1995).

The rate of photosynthesis at a given irradiance was lower in the afternoon than the morning (Figs. 3a, c, 4, 5). This photosynthetic inhibition is probably caused by high evaporative demand, or high temperature, or an intrinsic circadian rhythm, or a combination of effects (Figs. 5, 6d). The effect of afternoon depression was small compared to the effect of light, explaining only a few percent of the residual variance. Nonetheless, an accurate representation of this phenomenon may be needed to accurately predict the response of forest CO₂ exchange to climate.

The rate of photosynthesis at a given irradiance was reduced from May to September, apparently as a result of a decline in LAI (Fig. 8). This reduction in LAI preceded the drought (Fig. 1c, d), and appears to be genetically determined. The specific cue responsible for leaf senescence and leaf production was not identified, and understanding of the mechanisms controlling tropical phenology is poor (Wright 1996). An accurate representation of leaf phenology may be needed to accurately predict the response of forest CO₂ exchange to climate change. The seasonal pattern of LAI, and possibly the afternoon reduction in canopy photosynthesis, reflect anticipatory, feed-forward mechanisms, rather than responsive, feedback mechanisms. The seasonal trend in LAI appears to reflect an evolved pattern that anticipates the seasonal changes in precipitation. The afternoon decline in photosynthesis may be due in part to a circadian rhythm or a stomatal response that anticipate the onset of stress.

Belowground adaptations, including deep rooting and hydraulic lift, allowed the forest to avoid drought stress in 2000 (Figs. 1c, d, 2, 6b, 8). However, 2000 was a relatively wet year (Miller et al. 2004), and we cannot assume the forest avoids drought stress in dry years, such as those during strong El Niño periods. An improved understanding of the belowground adaptations to drought, and especially the effect of hydraulic lift, is needed to accurately predict the relationship between annual rainfall and drought stress. Feedback mechanisms, such as increased leaf senescence with extreme drought stress, may be important in drier years.

Changes in litter decomposition associated with drought were an important controller of the seasonal pattern of daily carbon balance (Figs. 9, 10, 11). The forest apparently accumulated carbon in the combined pool of live and dead leaves in the dry season, and lost carbon from this pool in the wet season. An understanding of the effects of drought on decomposition is

needed to accurately predict the sensitivities of daily, seasonal, and annual whole-ecosystem carbon balance to interannual climate variability.

ACKNOWLEDGMENTS

This work was supported by the U.S. National Aeronautics and Space Administration (Goddard NCC5-280). We thank Antonio Oviedo and Marcy Litvak for help installing equipment; Fernando Alves Leão and Roberto Cardoso for data collection; Dan Hodkinson, Lisa Zweede, and Bethany Reed for logistical support; IBAMA, NASA, and INPE for agency support; and many others who provided advice and support.

LITERATURE CITED

- Araújo, A. C., A. D. Nobre, B. Kruijt, J. Elbers, R. Dallarosa, P. Stefani, C. Randow, A. O. Manzi, A. D. Culf, J. H. C. Gash, R. Valentini, and P. Kabat. 2002. Dual tower long-term study of carbon dioxide fluxes for a central Amazonian rain forest: the Manaus LBA site. *Journal of Geophysical Research-Atmospheres* **107**:8090.
- Baldocchi, D. D., B. B. Hicks, and T. P. Meyers. 1988. Measuring biosphere-atmosphere exchanges of biologically related gases with micrometeorological methods. *Ecology* **69**: 1331-1340.
- Black, T. A., G. Den Hartog, H. H. Neumann, P. D. Blanken, P. C. Yang, C. Russell, Z. Nestic, X. Lee, S. G. Chen, R. Staebler, and M. D. Novak. 1996. Annual cycles of water vapour and carbon dioxide fluxes in and above a boreal aspen forest. *Global Change Biology* **2**:219-229.
- da Rocha, H. R., M. L. Goulden, S. D. Miller, M. C. Menton, L. D. V. O. Pinto, H. C. de Freitas, and A. M. e Silva Figueira. 2004. Seasonality of water and heat fluxes over a tropical forest in eastern Amazonia. *Ecological Applications* **14**:S22-S32.
- Fan, S.-M., M. L. Goulden, J. W. Munger, B. C. Daube, P. S. Bakwin, S. C. Wofsy, J. S. Amthor, D. R. Fitzjarrald, K. E. Moore, and T. R. Moore. 1995. Environmental controls on the photosynthesis and respiration of a boreal lichen woodland: a growing season of whole-ecosystem exchange measurements by eddy correlation. *Oecologia* **102**: 443-452.
- Fan, S.-M., S. C. Wofsy, P. S. Bakwin, D. J. Jacob, and D. R. Fitzjarrald. 1990. Atmosphere-biosphere exchange of CO₂ and O₃ in the central-Amazon-forest. *Journal Of Geophysical Research-Atmosphere* **95**:16 851-16 864.
- Grace, J., Y. Malhi, J. Lloyd, J. McIntyre, A. C. Miranda, P. Meir, and H. S. Miranda. 1996. The use of eddy covariance to infer the net carbon dioxide uptake of Brazilian rain forest. *Global Change Biology* **2**:208-217.
- Greco, S., and D. D. Baldocchi. 1996. Seasonal variations of CO₂ and water vapour exchange rates over a temperate deciduous forest. *Global Change Biology* **2**:183-197.
- Goulden, M. L., and P. M. Crill. 1997. Automated measurements of CO₂ exchange at the moss surface of a black spruce forest. *Tree Physiology* **17**:537-542.
- Goulden, M. L., B. C. Daube, S.-M. Fan, D. J. Sutton, A. Bazzaz, J. W. Munger, and S. C. Wofsy. 1997. Physiological responses of a black spruce forest to weather. *Journal of Geophysical Research* **102**:28 987-28 996.
- Goulden, M. L., J. W. Munger, S.-M. Fan, B. C. Daube, and S. C. Wofsy. 1996a. CO₂ exchange by a deciduous forest: response to interannual climate variability. *Science* **271**: 1576-1578.
- Goulden, M. L., J. W. Munger, S.-M. Fan, B. C. Daube, and S. C. Wofsy. 1996b. Measurements of carbon sequestration by long-term eddy covariance: methods and a critical evaluation of accuracy. *Global Change Biology* **2**:169-182.
- Hernandez Filho, P., Y. E. Shimabukuro, and D. C. L. Lee. 1993. Final report on the forest inventory project at the

- Tapajós National Forest. Instituto Nacional de Pesquisas Espaciais, São José dos Campos, SP, Brazil.
- Hollinger, D. Y., F. M. Kelliher, J. N. Byers, J. E. Hunt, T. M. McSeveny, and P. L. Weir. 1994. Carbon dioxide exchange between an undisturbed old-growth temperate forest and the atmosphere. *Ecology* **75**:134–150.
- Jarvis, P. G., and J. W. Leverenz. 1983. Productivity of temperate, deciduous and evergreen forests. Pages 233–280 in O. L. Lange, P. S. Nobel, C. B. Osmond, and H. Ziegler, editors. *Encyclopedia in plant physiology*. Volume 12D. *Physiological plant ecology IV*. Springer-Verlag, Berlin, Germany.
- Jarvis, P. G., J. M. Massheder, S. E. Hale, J. B. Moncrieff, M. Rayment, and S. L. Scott. 1997. Seasonal variation of carbon dioxide, water vapor, and energy exchanges of a boreal black spruce forest. *Journal of Geophysical Research-Atmospheres* **102**:28 953–28 966.
- Jones, H. G. 1992. *Plants and microclimate: a quantitative approach to environmental plant physiology*. Second edition. Cambridge University Press, Cambridge, UK.
- Keller, M., M. Palace, and G. Hurtt. 2001. Biomass in the Tapajós National Forest, Brazil—examination of sampling and allometric uncertainties. *Forest Ecology and Management* **154**:371–382.
- Koch, G. W., J. S. Amthor, and M. L. Goulden. 1994. Diurnal patterns of leaf photosynthesis, conductance and water potential at the top of a lowland rainforest in Cameroon: measurements from the Radeu de Cimes. *Tree Physiology* **14**:347–360.
- Larcher, W. 1995. *Physiological plant ecology: ecophysiology and stress physiology of functional groups*. Third edition. Springer-Verlag, Berlin, Germany.
- Li-Cor. 2000. LI-7000 CO₂/H₂O analyzer instruction manual. Publication number 0009–120. Li-Cor, Lincoln, Nebraska, USA.
- Liming, F. G. 1957. Homemade dendrometers. *Journal of Forestry* **52**:575–576.
- Malhi, Y., A. D. Nobre, J. Grace, B. Kruijt, M. G. P. Pereira, A. Culf, and S. Scott. 1998. Carbon dioxide transfer over a Central Amazonian rain forest. *Journal Of Geophysical Research-Atmospheres* **103**:31593–31612.
- McMillen, R. T. 1988. An eddy correlation technique with extended applicability to non-simple terrain. *Boundary-Layer Meteorology* **43**:231–245.
- Miller, S. D., M. L. Goulden, M. C. Menton, H. R. da Rocha, H. C. de Freitas, A. M. e Silva Figueira, and C. A. Dias de Sousa. 2004. Biometric and micrometeorological measurements of tropical forest carbon balance. *Ecological Applications* **14**:S114–S126.
- Nepstad, D. C., C. R. de Carvalho, E. A. Davidson, P. Jipp, P. Lefebvre, G. H. Negreiros, E. D. da Silva, T. Stone, S. Trumbore, and S. Vieira. 1994. The role of deep roots in the hydrological and carbon cycles of Amazonian forests and pastures. *Nature* **372**:666–669.
- Rice, A. H., E. H. Pyle, S. R. Saleska, L. Hutyrá, M. Palace, M. Keller, P. D. de Carmargo, K. Portilho, D. F. Marques, and S. C. Wofsy. 2004. Carbon balance and vegetation dynamics in an old-growth Amazonian forest. *Ecological Applications* **14**:S55–S71.
- Ruimy, A., P. G. Jarvis, D. D. Baldocchi, and B. Saugier. 1995. CO₂ fluxes over plant canopies and solar radiation: a review. *Advances in Ecological Research* **26**:1–68.
- Savage, K. E., and E. A. Davidson. 2001. Interannual variation of soil respiration in two New England forests. *Global Biogeochemical Cycles* **15**:337–350.
- Williams, M., Y. Malhi, A. D. Nobre, E. B. Rastetter, J. Grace, and M. G. P. Pereira. 1998. Seasonal variation in net carbon exchange and evapotranspiration in a Brazilian rain forest: a modelling analysis. *Plant, Cell and Environment* **21**:953–968.
- Wofsy, S. C., M. L. Goulden, J. W. Munger, S.-M. Fan, P. S. Bakwin, B. C. Daube, S. L. Bassow, and F. A. Bazzaz. 1993. Net exchange of CO₂ in a mid-latitude forest. *Science* **260**:1314–1317.
- Wright, S. J. 1996. Pages 440–460 in S. S. Mulkey, R. L. Chazdon, and A. P. Smith, editors. *Tropical forest plant ecophysiology*. Chapman and Hall, New York, New York, UK.
- Wright, S. J., and F. H. Cornejo. 1990. Seasonal drought and leaf fall in a tropical forest. *Ecology* **71**:1165–1175.
- Zotz, G., and K. Winter. 1996. Pages 89–113 in S. S. Mulkey, R. L. Chazdon, and A. P. Smith, editors. *Tropical forest plant ecophysiology*. Chapman and Hall, New York, New York, UK.